

Supplementary Materials and Methods:

Non-human primate (NHP) Study Design and Transplant Strategy

Both REGN421x1 and REGN421x3 cohorts used half-sibling major histocompatibility complex (MHC) haplo-identical donor and recipient pairs (data file S1). Experiments were performed using our previously described strategy (13-16). Briefly, apheresis was performed after Granulocyte-Colony Stimulating Factor (G-CSF) mobilization (Amgen, 50 µg/kg for 5 days), and an unmanipulated apheresis product was transplanted into allogeneic hematopoietic cell transplantation (allo-HCT) recipients. The transplanted total nucleated cell dose and CD3⁺ T cell dose are shown in data file S1. The pre-HCT preparative regimen consisted of total body irradiation of 10.4 cGy given in two fractions per day for two days. Irradiation was delivered using a linear accelerator Varian Clinac 23EX with a tissue-adjusted dose rate of 7 cGy/min or gamma-irradiation with a Cobalt-60 isotope at a tissue-adjusted dose rate of 5.5 cGy/min. All transplants were performed with a central venous catheter placed for the length of the experiment. Antibacterial prophylaxis including Vancomycin (target serum concentration of 5 to 20 µg/mL) as well as Ceftazidime, both administered by central catheter, and Enrofloxacin ('Baytril'), administered intramuscularly, was given to all recipients with neutrophil counts < 500 cells/µL. Antiviral prophylaxis consisting of acyclovir [10 mg/kg intravenously (IV) daily] and cidofovir (5 mg/kg IV weekly), as well as antifungal prophylaxis (fluconazole 5mg/kg orally or IV daily), were also employed. Leukoreduced (LRF10 leukoreduction filter, Pall Medical) and irradiated (2200 rad) platelet-rich plasma or whole blood was given for a peripheral blood platelet count of $\leq 50 \times 10^3$ per µL or a hemoglobin <9 g/dL, respectively, or upon clinically meaningful hemorrhage. Blood product support adhered to ABO matching principles. The acute graft-versus-host disease (aGVHD) clinical score was assessed daily and summarized weekly for allo-HCT recipients, as described (13-16). Briefly, the aGVHD clinical score increases with gastrointestinal tract (GI)-specific (diarrhea), liver-specific (hyperbilirubinemia) and skin-specific abnormalities (extent and character of rash). The studies

described here focused on the natural history of aGVHD that developed during prophylaxis, so that animals were not given supplementary treatment when GVHD was diagnosed. Rather, when pre-defined clinical endpoints were met (based on the BBRM and WPNRC veterinary standard operating procedures), animals were euthanized and terminal analysis was performed. Thus, survival was directly related to severity of clinical GVHD. Histopathologic scoring for GVHD was performed by an expert in GVHD histopathology (A.P.M.) using a previously validated semi-quantitative scoring system (Grades 0.5 to 4). The pathologist was blinded to treatment cohorts during scoring.

GVHD prophylaxis regimens

Two DLL4 blockade strategies were evaluated. The first cohort received one dose of good manufacturing practices (GMP) grade anti-DLL4 blocking antibodies REGN421 (Regeneron) on day 0 at 3 mg/kg, 3 hours prior to infusion of the donor leukapheresis product. REGN421 (also called enoticumab) was developed as a fully humanized IgG1 monoclonal antibody that binds human or NHP DLL4 (but not mouse DLL4) with sub-nanomolar affinity and inhibits DLL4-mediated Notch signaling, as described (33). The REGN421 dose was selected based on past pharmacokinetic measurements showing therapeutic in vivo concentrations in healthy humans (32). The second cohort of animals received 3 mg/kg REGN421 on days 0, +7 and +14 relative to the HCT (the day 0 dose was also given 3 hours before the leukapheresis product). The primary endpoint for REGN421-receiving cohorts was the proportion of animals surviving to 60 days post-transplant. No treatment for aGVHD was provided in this study; therefore, the clinical endpoints were unaffected by GVHD therapy. Pharmacokinetic studies of REGN421 were performed with blood obtained longitudinally from REGN421-treated recipients, using an ELISA developed at Regeneron (32).

Chimerism determination

Whole blood, bone marrow and T cells (sorted by flow cytometry as CD3⁺CD20⁻) were analyzed for donor chimerism based on microsatellite markers. Chimerism analysis was performed at the UC Davis veterinary genetics laboratory. Analysis was performed as previously described (14).

NHP necropsy and tissue processing

Animals were humanely euthanized followed by perfusion with PBS (0.5 L/kg body weight), necropsy and tissue harvest. Peripheral blood mononuclear cells (PBMCs) were isolated using Ficoll-Paque PLUS gradient separation and standard procedures. Lymph nodes, spleen, and bone marrow (from long bones) were mechanically disrupted by grinding through a metal strainer, followed by filtering through nylon 70 µm and 40 µm cell strainers. Lungs, liver, jejunum, colon, and kidney samples were cut into small pieces, then digested using 150 KU DNase (Sigma-Aldrich) with 1 mg/mL type I collagenase (Invitrogen) (lungs, liver, and kidney) or 150 KU DNase (Sigma-Aldrich) with 50 µg/mL Liberase TL (Roche; colon and jejunum) at 37°C for 1 hour with shaking, followed by passing through a metal strainer, and then 100 µm, 70 µm and 40 µm nylon cell strainers. The cell suspension was further purified using a double-layer Percoll (GE Healthcare) gradient separation. The leukocyte fraction was collected at the interphase between 70% and 30% Percoll. Cells were washed and immediately analyzed, or cryopreserved in 10% DMSO/90% FBS and stored in liquid nitrogen.

Multiparameter flow cytometry on NHP samples

Samples were processed as described (13) and either analyzed fresh or from cryopreserved samples. Cryopreserved samples were washed with PBS and incubated with 200 µL 1:100 LIVE/DEAD Aqua (Invitrogen) for 20 minutes at 37°C using 96-well cell culture plates. After viability staining, cells were washed with staining buffer (PBS + 2% heat-inactivated FBS) and stained with antibody cocktails against extracellular targets (data file S8) at 4°C for 20 minutes,

followed by washing with staining buffer. Fresh samples were washed with staining buffer and stained with extracellular antibody cocktails without prior viability staining.

Samples stained with extracellular antibodies only were fixed with 1X BD Stabilizing Fixative and run within 24 hours after staining. Samples requiring intracellular staining were incubated in 250 μ L Cytotfix/Cytoperm solution (BD Biosciences) at 22°C for 20 minutes. This was followed by washing with 1X Perm/Wash buffer (BD Biosciences) and incubation with intracellular antibody cocktails mixed in 50 μ L of the 1X Perm/Wash buffer at 4°C for 30 minutes (data file S8). These samples were washed and analyzed within 24 hours after staining. Samples requiring intranuclear staining were incubated in 250 μ L Foxp3 fixation buffer (BioLegend) at 22°C for 20 minutes, followed by washing with Foxp3 wash buffer (BioLegend). Samples were then incubated with intranuclear antibody cocktails mixed in 50 μ L of the Foxp3 wash buffer at 4°C for 30 minutes (data file S8). These samples were washed and analyzed within 24 hours after staining. Flow cytometry was performed on a BD FACS LSRFortessa and analyzed with FlowJo v.10 in an unblinded manner.

T cell sorting

Sorting was performed using a FACSAria or FACSJazz Cell Sorter (BD Biosciences). CD3⁺ T cells were sorted from the blood of healthy controls, allo-HCT recipients at day 15 \pm 1 post-transplant (as survival permitted), and allo-HCT recipients at terminal analysis. T cells defined as CD3⁺CD20⁻ lymphocytes were >90% pure based on post-sorting flow cytometric analysis, as described (15, 16).

NHP microarray and data analysis

Following T cell purification, RNA was stabilized with RLT buffer (Qiagen) supplemented with 1% (vol/vol) beta-mercaptoethanol (Sigma). RNA was purified using RNEasy Columns

(Qiagen). RNA was quantified using a Nanodrop Spectrophotometer (Thermo Fisher) and purity was confirmed with RNA 6000 Nano kits (Agilent). Purified RNA was sent to the Vanderbilt Technologies for Advanced Genomics Core and to the Oregon Health Sciences University Gene Profiling Shared Resource, where RNA quantity and quality were verified, followed by cDNA/cRNA synthesis, and target hybridization to GeneChip Rhesus Macaque Genome Array (Affymetrix). Resultant fluorescent signals were processed and normalized using the Robust Multichip Averaging (RMA) Method (63). Microarrays were processed in 10 batches, with all batches containing samples from healthy controls and transplanted animals. The “ComBat” algorithm was implemented to adjust for batch effects (64) and probe-sets containing low signal-to-noise measurement were filtered out to enhance statistical testing power (65). Probe-sets were annotated using 1) annotation files from (66); 2) annotation files from the chip manufacturer (release 33); and 3) data provided by Ingenuity Systems (Ingenuity Systems, www.ingenuity.com) for the small number of probe-sets not annotated by the chip manufacturer. Principal Component Analysis (PCA) was applied to summarize gene array variance using the Bioconductor (67) MADE4 package (68). Analysis of gene differential expression (DE) was performed using an empirical Bayes moderated t-statistic, with a cutoff of 0.05, corrected for multiple hypothesis testing using Benjamini-Hochberg procedure (absolute fold change cutoff >1.4 with the limma package) (69).

Gene Set Enrichment Analysis (GSEA)

GSEA was performed using GSEA 4.1.0 tool (70, 71) and gene sets from the Molecular Signatures Database v7.4 on aggregate sample data from each cohort as a whole. Gene sets were ranked using a signal to noise ratio difference metric with 1000 permutations of gene set labels.

Functional annotation of genes and pathway enrichment analysis using Metascape

Functional annotation and pathway enrichment analysis was performed using the Metascape tool (metascape.org) (44). First, Rhesus macaque genes were mapped to human orthologs. Then, all statistically enriched terms from gene ontology (GO), KEGG, Biocarta, Reactome, HALLMARK, CORUM, canonical pathways, WikiPathways databases, accumulative hypergeometric p-values and enrichment factors were calculated and used for filtering. Remaining terms were hierarchically clustered into a tree based on Kappa-statistical similarities among their gene memberships. 0.3 kappa score was applied as the threshold to cast the tree into term clusters. The terms within each cluster are shown in data files S5 and S6. We then selected a subset of representative terms from this cluster and converted them into a network layout. More specifically, each term was represented by a circle node, with its size proportional to the number of input genes falling into that term and its color representing its cluster identity (nodes of the same color belong to the same cluster). Terms with similarity scores >0.3 were linked by an edge (the thickness of the edge representing the similarity score). The network was visualized with Cytoscape (v3.1.2) (72) with “force-directed” layout and with edge bundled for clarity. One term from each cluster was selected to have its term description shown as label.

Analysis of upstream regulators using Ingenuity Pathway Analysis

Pathway analysis on differentially expressed genes was performed using Ingenuity Pathway Analysis (IPA; <https://www.qiagenbioinformatics.com/products/ingenuity-pathway-analysis/>). Upstream regulators (limited to the following terms: complex, cytokine, group, growth factor, G-coupled receptor, kinase, ligand-dependent nuclear receptor, micro-RNA, mature micro-RNA, phosphatase, transmembrane receptor, transcriptional regulator, and translational regulator) were considered activated or inhibited if enrichment z-scores were greater than 1.25 or less than -1.25, respectively. p values were <0.05 using Benjamini-Hochberg-corrected t-tests.

Immunofluorescence analysis of NHP colon

Colon specimens were collected at terminal analysis. Tissues were fixed in 10% buffered formalin and embedded in paraffin. Tissue sections (4 μm) were obtained using a microtome, deparaffinized and then antigen retrieval was performed at 120°C for 30 seconds (2100 Retriever, Aptum Biologics). Slides were blocked using goat serum in PBS containing 0.2% bovine serum albumin (BSA) for 1 hour and stained for 1 hour at 37°C using primary antibodies: rat anti-CD3 (Biorad, Cat# MCA1477) and mouse anti-Ki67 (Dako, Cat# M724029-2). The following fluorescently labeled secondary antibodies were used to stain tissues for 1 hour at 37°C: goat anti-rat Alexa Fluor (AF) 488 (Invitrogen, Cat# A-11006) and goat anti-mouse IgG1 AF647 (Invitrogen, Cat# A-21240). Sections were washed, stained with Hoechst (2 $\mu\text{g}/\text{mL}$, Invitrogen, Cat# H3570) and mounted using Prolong Gold (Invitrogen). Images were acquired using a Zeiss Axio Scan Z1 microscope and tile stitching was performed using the ZEN Blue software (Carl Zeiss).

Image processing, modeling and quantification of cell populations was performed with Imaris v9.7 (Bitplane AG). Among all tile scan images collected initially (HD=8, NoRx=7, REGN421=9), 5 animals per group presented staining of good quality, with reliable signal for all antibodies and absence of autofluorescence. From all tile scan images, 2 to 6 representative areas per animal were cropped, and 1 to 3 representative images with well-preserved tissue structure were selected for analysis (total 33 images, with 11 images per group). These images were deidentified and quantification analysis was performed on Imaris in a blinded fashion by a single investigator (D.G.A.). Each channel was processed separately, and cells were modeled as spots based on Hoechst nuclear staining. Data were plotted using Prism (GraphPad) and statistically significant differences were determined using Kruskal-Wallis multiple comparison test.

Mice

C57BL/6 (B6, H-2^{b/b}, Thy1.2⁺) and C57BL/6-Thy1.1 mice (B6-Thy1.1, H-2^{b/b}, Thy1.1⁺) were originally from The Jackson Laboratory (Bar Harbor, ME) and bred at the University of Pennsylvania. C57BL/6 x BALB/c F1 (#100007, CBF1, H-2^{b/d}, Thy1.2⁺) and congenic B6.SJL-Ptprc^a mice (#002014, B6-CD45.1, H-2^{b/b}, Thy1.2⁺) were from The Jackson Laboratory. B6 *Cd4-Cre;ROSA^{DNMAML}* mice (expressing the pan-Notch inhibitor DNMAML fused to GFP in mature CD4⁺ and CD8⁺ T cells under the control of the *ROSA26* promoter) were described previously (19, 61). *Cd4-Cre⁻* or *Cd4-Cre⁺* mice were used as controls, as *Cd4-Cre* expression alone had no impact on all Notch-sensitive T cell endpoints after allo-HCT (fig. S10). *Ccl19-Cre⁺ Dll1^{ff} Dll4^{ff}* mice, inactivating *Dll1* and *Dll4* in secondary lymphoid organ fibroblastic reticular cells, have been described (24, 43). *Ccl19-Cre⁻* or *Ccl19-Cre⁺* mice were used as controls, as we previously showed that *Ccl19-Cre* expression alone had no impact on Notch-sensitive endpoints after allo-HCT (24). *Itgb1^{ff}* mice on a mixed B6;129 background (H-2^{b/b}) were from The Jackson Laboratory (#004605) (62). *Itgb1^{ff}* mice were crossed to *Cd4-Cre;ROSA^{DNMAML}* mice to generate *Cd4-Cre;Itgb1^{ff}* vs. *Cd4-Cre;Itgb1^{ff};ROSA^{DNMAML}* mice. For bone marrow transplantation experiments, co-housed littermate controls were used as donors and recipients at the University of Pennsylvania, per protocols approved by the University of Pennsylvania's Office of Regulatory Affairs.

Mouse tissue processing

Single cell suspensions from spleen, mesenteric lymph nodes, or pooled peripheral lymph nodes (cervical, brachial, axial, inguinal) were prepared by physical disruption through 70 μ m cell strainers. Single cell suspensions were prepared from liver as described (17). Intestinal lamina propria and intestinal epithelium was prepared as described with slight modifications (19). Briefly, intestines were washed and cut longitudinally after removal of Peyer's patches from the small intestine. Fragments (0.5 to 1 cm) of intestine were cleaned of mucus and feces

and incubated in PBS with 2mM EDTA and 5% FBS without dithiothreitol for 45 minutes with shaking at 37°C. Supernatant was passed through 100µM MACS SmartStrainers (Miltenyi Biotec) and collected as intestinal epithelial lymphocyte (IEL) fraction. For isolation of lamina propria lymphocytes (LPL), the remaining tissue was incubated in RPMI-1640/FBS 10% with 1mg/mL collagenase IV (Gibco) for 20 minutes with shaking at 37°C. The resulting tissue was vigorously pipetted and supernatant passed through 100µM MACS SmartStrainers. Debris were removed using 40%:80% Percoll gradient separation.

Multiparameter flow cytometry on mouse samples.

Samples were washed with PBS and incubated with 200 µL 1:400 LIVE/DEAD LIVE/DEAD Aqua (Invitrogen) for 30 minutes at 4°C using 96-well U-bottom plates. After viability staining, cells were washed in PBS + 2% heat-inactivated FBS twice, and stained with antibody cocktails mixed in 50 µL of PBS + 2% FCS against extracellular targets (data file S8) for 30 minutes at 4°C. Fc receptors were blocked with unlabeled anti-mouse CD16/32 (BioLegend). Samples requiring intranuclear staining were subsequently incubated in 200 µL Foxp3 fixation/permeabilization buffer (BioLegend) at 22°C for 30 minutes. Samples were then washed with Foxp3 wash buffer (BioLegend) twice and then incubated with intranuclear antibody cocktails mixed in 50 µL of the Foxp3 wash buffer at 22°C for 30 minutes (data file S8). These samples were washed and analyzed within 12 hours after staining. Flow cytometry was performed on either a 4 or 5-laser BD Fortessa (Becton Dickinson) or a 5-laser BD FACSymphony A3 (Becton Dickinson) and analyzed in FlowJo v.10 (Becton Dickinson) in an unblinded manner.

Supplementary Figures

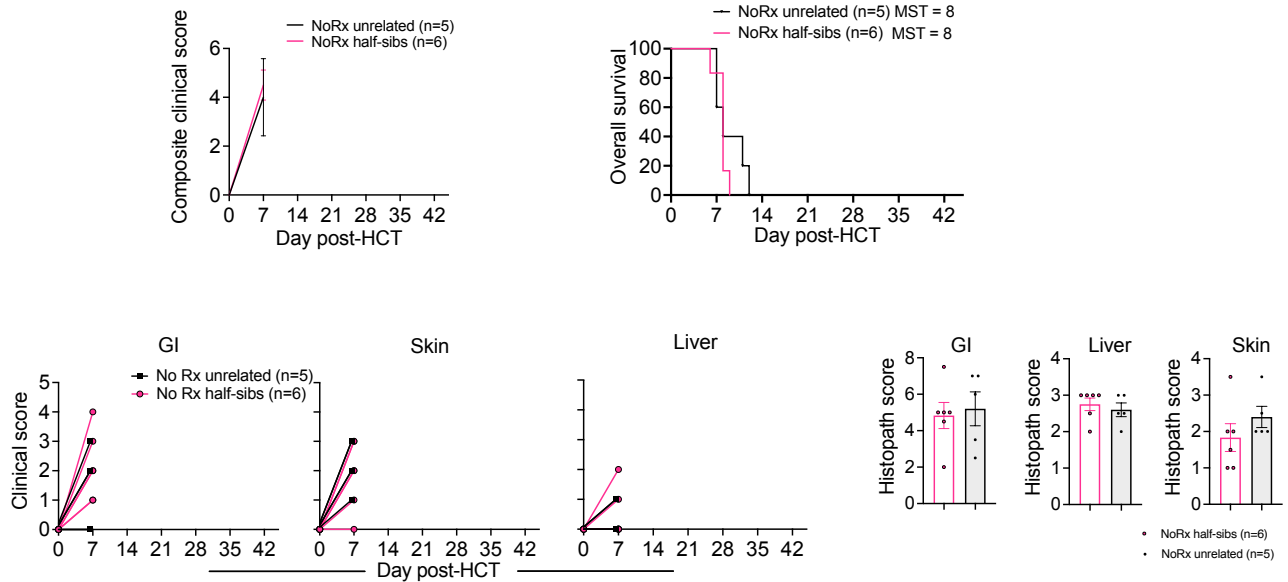
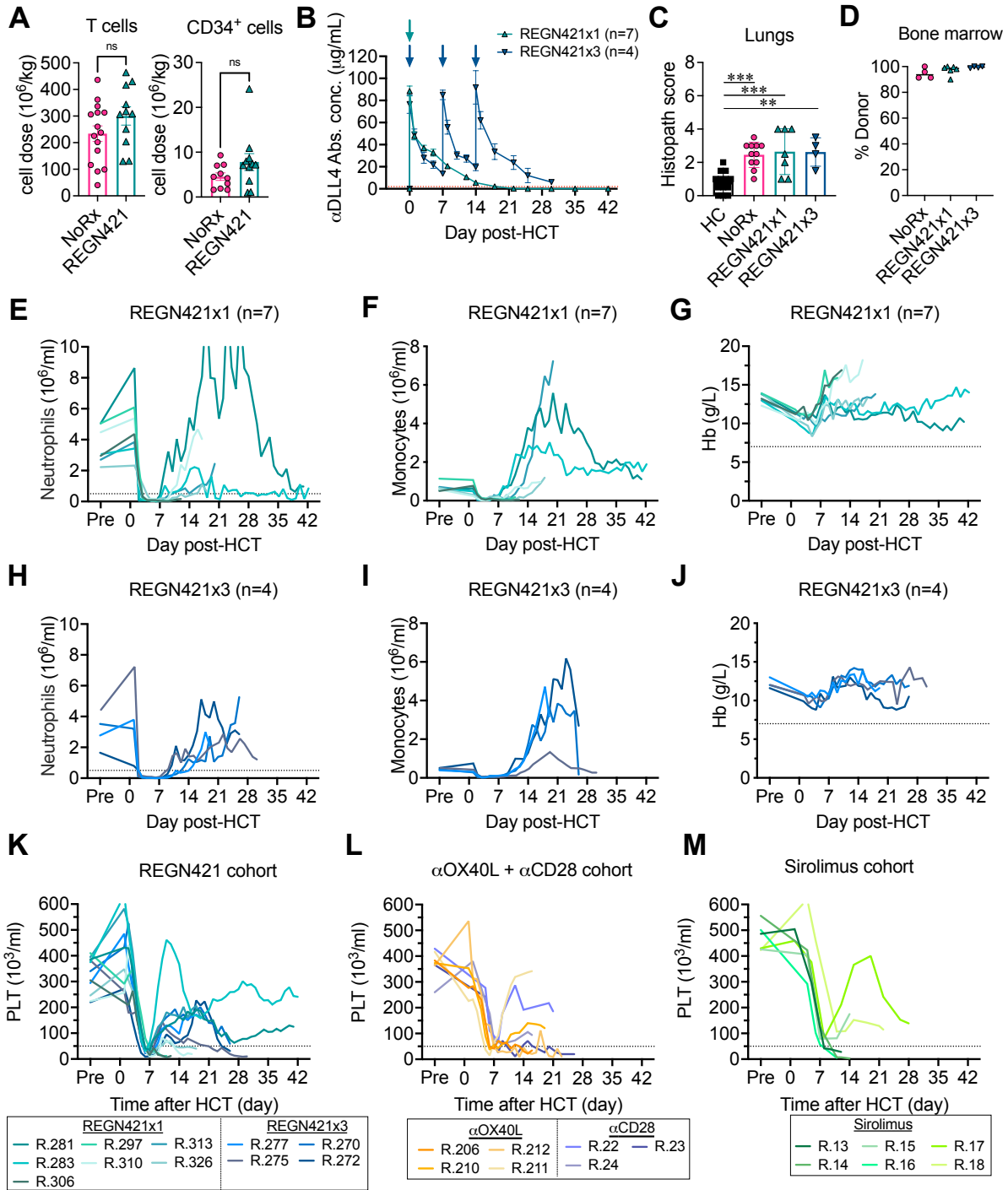


Figure S1. No difference was observed in the clinical outcome of NHP recipients of untreated unrelated versus half-sibling haploidentical hematopoietic cell transplantation. The figure shows composite clinical score, overall survival, organ-specific clinical GVHD scores, and organ-specific histopathological scores in two subgroups of haploidentical recipients receiving untreated transplantation (NoRx) from unrelated (n=5) or half-sibling donors (n=6).



N

Cohort	Cohort size	Euthanized before PMN engraftment	%	Refractory thrombocytopenia or bleeding complications	%
αOX40L	4	2	50%	2	50%
αCD28	3	0	0%	1	33%
Sirolimus	6	3	50%	3	50%
REGN421x3	4	0	0%	2	50%
REGN421x1	7	2	29%	4	57%

Figure S2. Pharmacokinetics of REGN421 in the allo-HCT NHP model and hematopoietic reconstitution of REGN421-prophylaxed allo-HCT recipients. (A) Numbers of CD3⁺CD20⁻ T cells and CD34⁺ progenitor cells in the donor grafts of the NoRx and REGN421 experimental cohorts. ns, not significant (Student's t-test). (B) Systemic concentrations of REGN421 following the single or triple dosing regimen (REGN421x1, REGN421x3). (C) Histopathological aGVHD scores for lungs. **p<0.01, ***p<0.001 using one-way ANOVA with Tukey post-hoc test. HC, healthy control. (D) Percent donor chimerism in the bone marrow at the time of terminal analysis. (E to J) Absolute numbers of neutrophils (E and H), monocytes (F and I), and hemoglobin concentrations (Hb, G and J) are shown for the REGN421x1 and REGN421x3 cohorts. (K) Platelet (PLT) numbers are shown for the REGN421x1 and REGN421x3 cohorts. (L and M) As a comparison, platelet counts from previously reported NHP allo-HCT experiments with aOX40L/CD28. The dashed dotted lines indicate the threshold of neutropenia requiring additional antibacterial prophylaxis (for E and H) as well as anemia (for G and J) and thrombocytopenia (for K, L and M) requiring blood transfusion. (N) Table reporting the number and percentage of NHP recipients meeting early euthanasia criteria before neutrophil engraftment (polymorphonuclear cells, PMN), as well as the rate of refractory thrombocytopenia and bleeding complications across multiple treatment groups. The incidence of early complications was similar across experiments.

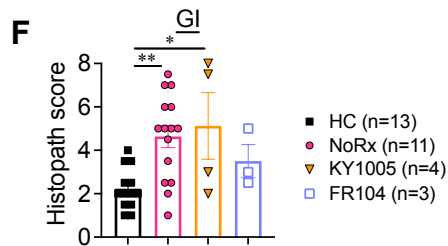
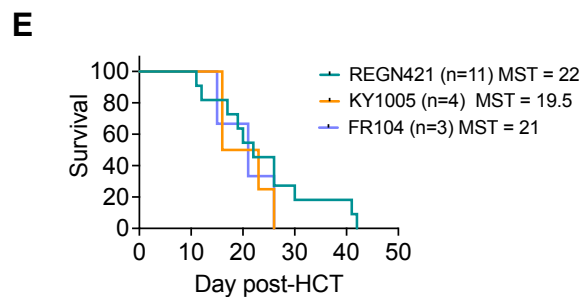
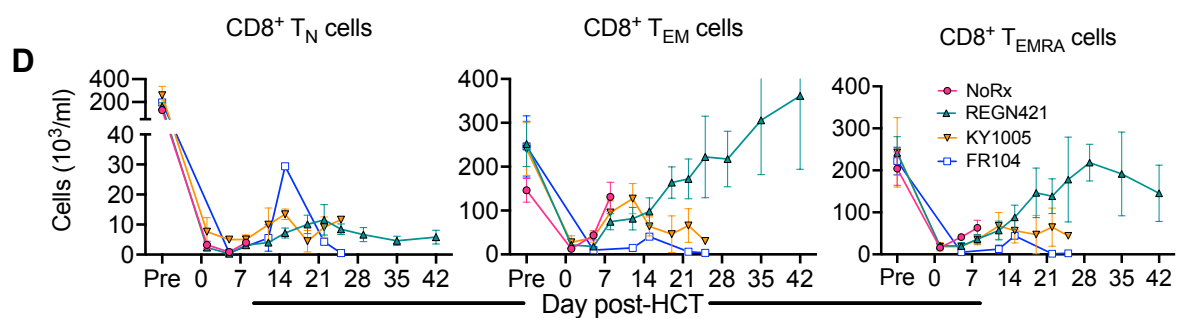
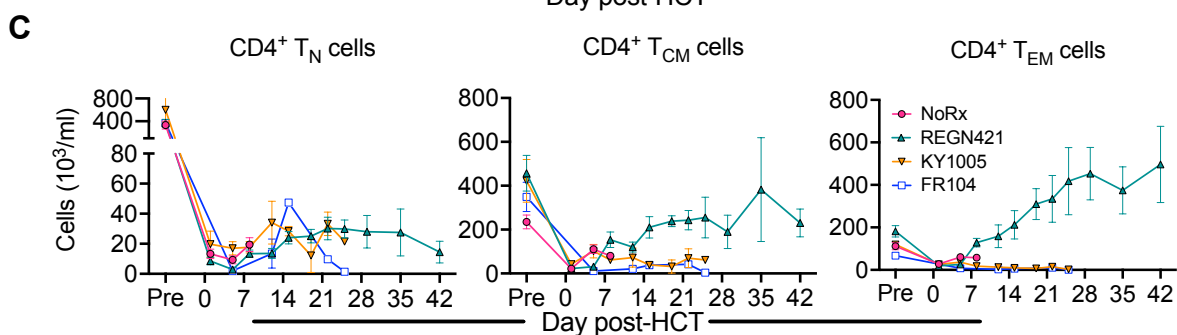
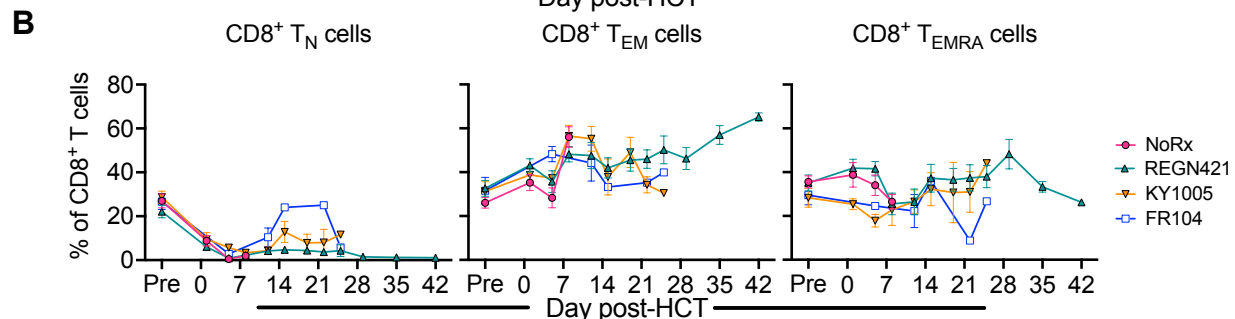
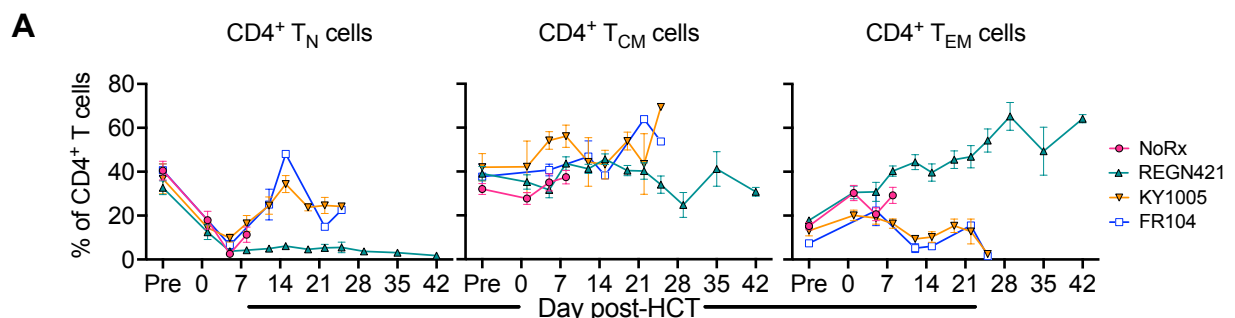


Figure S3. T cell reconstitution in the REGN421 experimental cohort and comparison to other single agent interventions. (A and B) Frequencies of CD4⁺ (A) and CD8⁺ (B) T cells with CD45RA⁺CCR7⁺CD95⁻ naïve (T_N), CD45RA⁻CCR7⁺ central memory (T_{CM}), and CD45RA⁻CCR7⁻ effector-memory phenotypes (T_{EM} and T_{EMRA}) in the peripheral blood of allo-HCT recipients from distinct treatment groups, as indicated. No Rx: no prophylaxis controls; REGN421: combined cohort of NHP recipients treated with 1 or 3 doses of the anti-DLL4 REGN421; KY1005: OX40L blockade; FR104: CD28 blockade (12-13) **(C and D)** Absolute numbers of the peripheral blood CD4⁺ (C) and CD8⁺ (D) T cell subsets corresponding to the relative numbers in (A) and (B). **(E)** Overall survival of allo-HCT recipients in the combined REGN421 cohort (recipients that received either one or three doses of REGN421, n=11), anti-CD28/FR104 (purple, n=3) and anti-OX40L/KY1005 experimental cohorts (orange, n=4). **(F)** Histopathological aGVHD scores for GI tract in the combined REGN421 cohort (recipients that received either one or three doses of REGN421, n=11), anti-CD28/FR104 (purple, n=3), and anti-OX40L/KY1005 experimental cohorts (orange, n=4) *p<0.05, **p<0.01 using one-way ANOVA with Tukey post-hoc test.

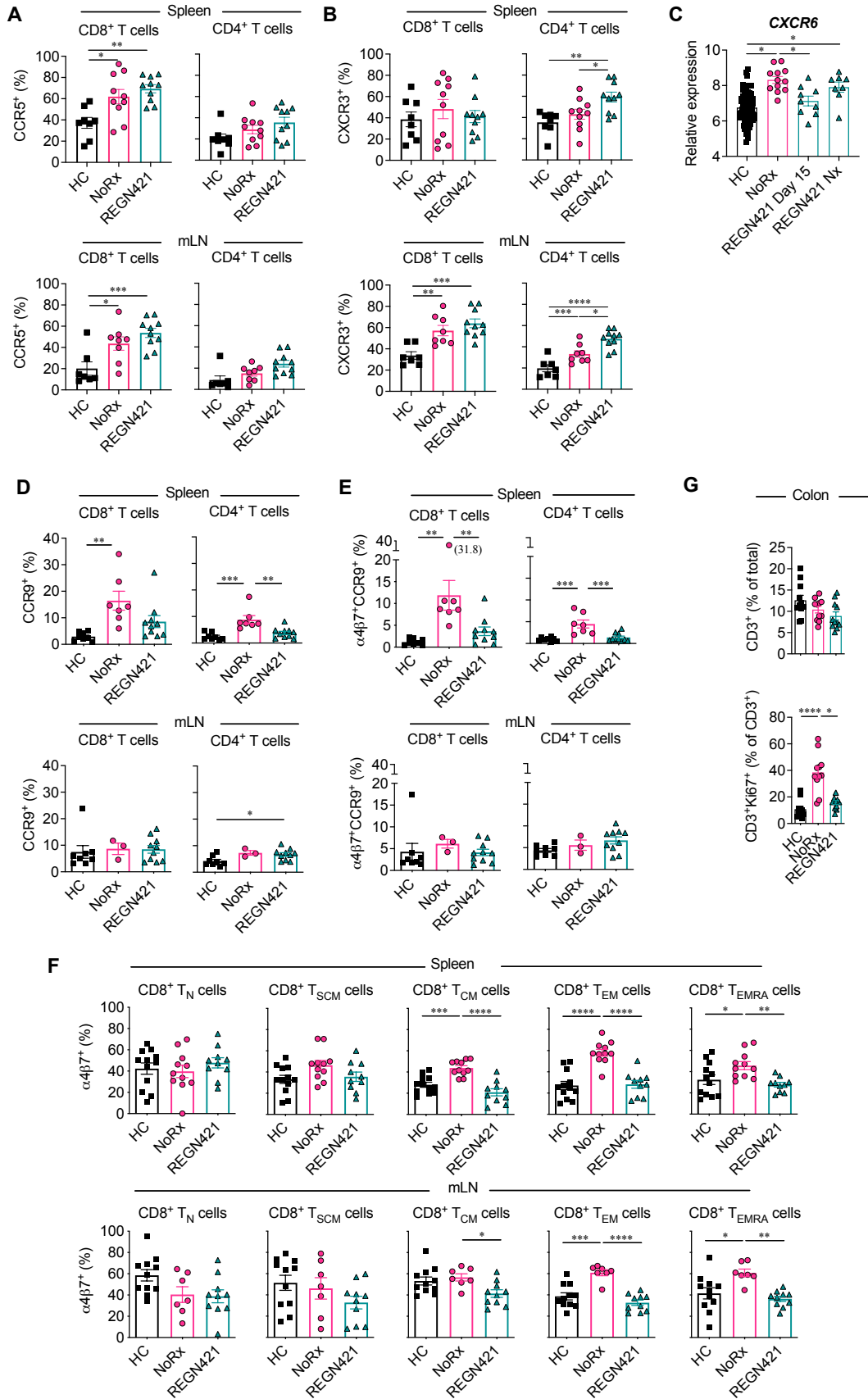


Figure S4. Expression of chemokine receptors on CD8⁺ and CD4⁺ T cells. (A and B)

Frequency of CCR5⁺ (A) or CXCR3⁺ (B) CD8⁺ and CD4⁺ T cells in the spleen and mesenteric lymph nodes (mLN) of healthy control animals (n=7 to 8 depending on organ), as well as in the allo-HCT recipients from NoRx aGVHD (n=8 to 10 depending on the organ) and REGN421 (n=10) cohorts. *p<0.05, **p<0.01, ***p<0.001, ****p<0.0001, using one-way ANOVA with Tukey post-hoc test. (C) Relative abundance of *CXCR6* mRNA in CD3⁺CD20⁻ T cells from peripheral blood, sorted on day +15 after allo-HCT or at the time of terminal analysis (Nx). *q<0.01 using Benjamini-Hochberg test. (D and E) Frequency of CCR9⁺ (D) or α 4 β 7⁺CCR9⁺ (E) CD8⁺ and CD4⁺ T cells in the spleen and mLN of healthy control animals (n=8 depending on organ), as well as in the allo-HCT recipients from NoRx aGVHD (n=3 to 7 depending on organ) and REGN421 (n=10) cohorts. *p<0.05, **p<0.01, ***p<0.001 using one-way ANOVA with Tukey post-hoc test. (F) Frequency of α 4 β 7⁺ T cells among individual CD8⁺ T cells subsets identified in the spleen and mLN as indicated. T_N: naïve, CD45RA⁺CCR7⁺CD95⁻; T_{SCM}, stem cell memory CD45RA⁺CCR7⁺CD95⁺; T_{CM}, central memory CD45RA⁻CCR7⁺; T_{EM}, effector memory CD45RA⁻CCR7⁻; T_{EMRA}, terminal effector CD45RA⁺CCR7⁻. *p<0.05, **p<0.01, ***p<0.001, ****p<0.0001, using one-way ANOVA with Tukey post-hoc test. (G) Proportion of CD3⁺ T cells, as well as Ki67⁺ cells among CD3⁺ T cells, in the colon as assessed by immunofluorescence imaging and quantified using the Imaris software (n=11 images from 5 animals per group). *p<0.05, ****p<0.0001 using a Kruskal-Wallis multiple comparison test.

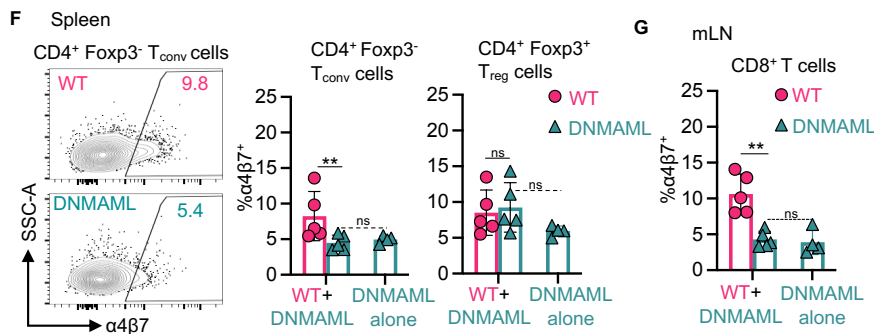
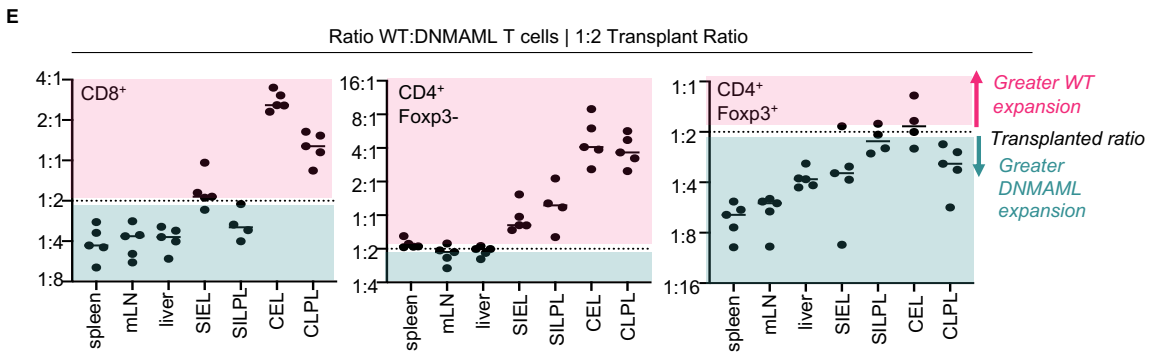
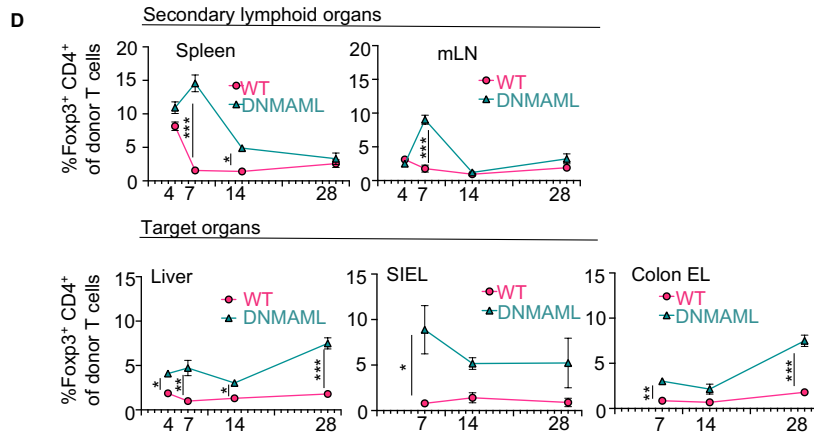
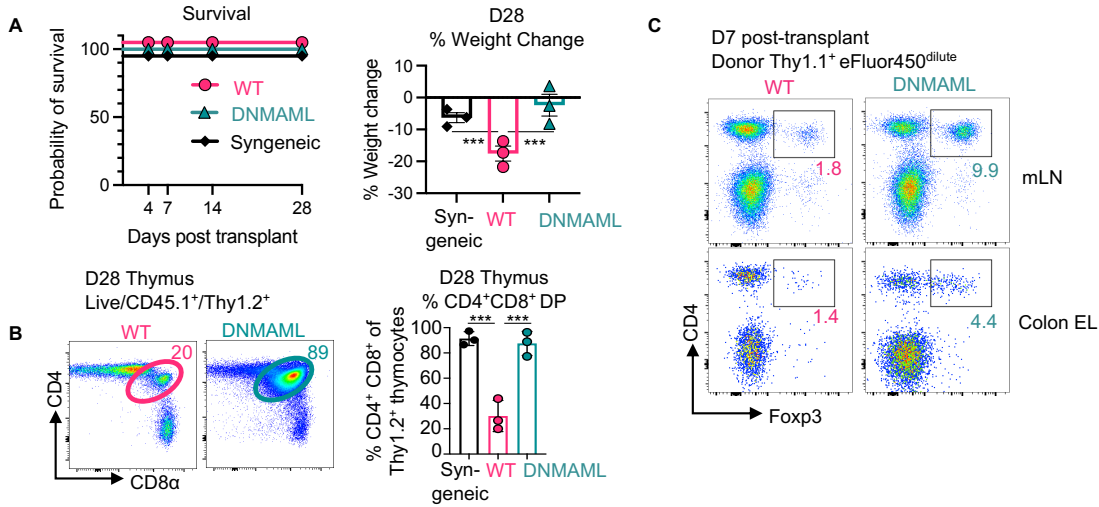


Figure S5. Cell-intrinsic canonical Notch signals control $\alpha 4\beta 7$ expression and gut-homing potential in alloreactive T cells. (A to D) These data are related to the experiments depicted in Fig. 5A to C. (A) Survival and weight change at day 28 post-transplant. (B) Representative flow cytometry plots showing the frequency of CD4⁺CD8⁺ cells among newly formed CD45.1⁺Thy1.2⁺ thymocytes at day 28 post-transplant, summarized on the right (as a readout for thymic GVHD). (C and D) Flow cytometry plots (C) showing the frequency of Foxp3⁺CD4⁺ regulatory T (T_{reg}) cells among donor T cells in mLN and colon epithelial lymphocytes (EL), as summarized in multiple organs across multiple timepoints in (D). (E) Similar experiment as in Fig. 5F, but recipients were transplanted with a 1:2 ratio of wild type:DNMAML T cells. Relative accumulation of wild type to DNMAML T cells was calculated in each organ fraction. (F and G) Flow cytometric analysis of $\alpha 4\beta 7$ expression in donor Foxp3⁻CD4⁺ conventional T (T_{conv}) cells from recipients receiving wild type and DNMAML T cells (1:1) versus DNMAML T cells alone in spleen (F) and mLN (G). *p<0.05, **p<0.01, ***p<0.001, ns, not significant as determined by one-way ANOVA with Tukey's post-hoc test. SIEL, small intestine epithelial lymphocytes; SILPL, small intestine lamina propria lymphocytes; CEL, colon epithelial lymphocytes; CLPL, colon lamina propria lymphocytes; SSC-A, side scatter area.

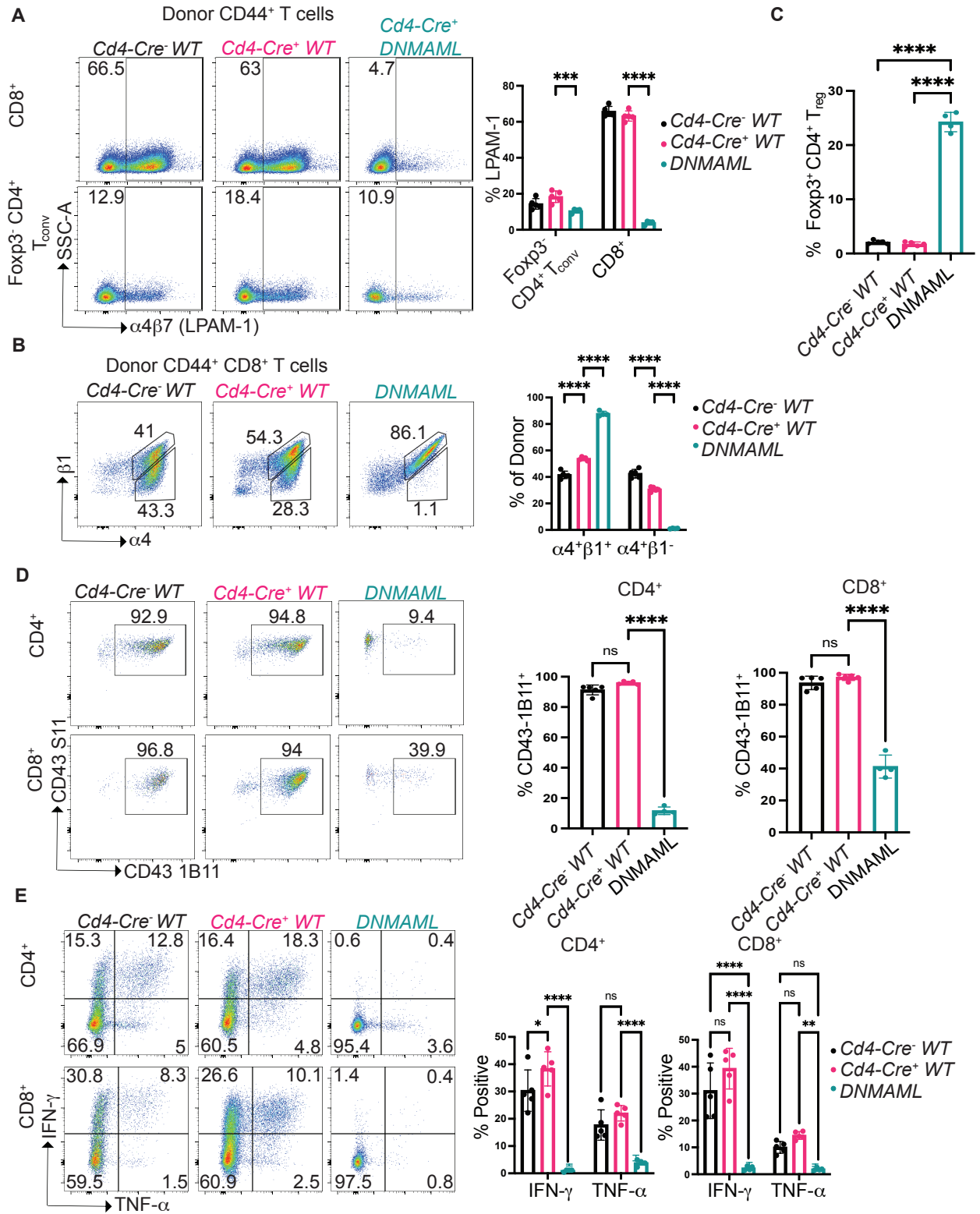


Figure S6. *Cd4-Cre* expression alone exerts no or only minimal impact on Notch-dependent T cell endpoints after allo-HCT. Allo-HCT was performed using lethally irradiated C57BL/6 x BALB/c recipients (CBF1, 11 Gy) and C57BL/6 donors, with or without expression of *Cd4-Cre* or *Cd4-Cre* and the pan-Notch inhibitor DNMA1L in mature T cells (*Cd4-Cre*^{neg} wild-type [WT] versus *Cd4-Cre*⁺ versus *Cd4-Cre*⁺ *ROSA*^{DNMA1L}, abbreviated DNMA1L) (n=4 to 5 per group). **(A)** $\alpha 4\beta 7$ (LPAM-1) expression among CD44⁺ activated donor-derived T cells in the spleen at day 4.5 after allo-HCT. Representative flow cytometry plots and quantification are shown for CD8⁺ and Foxp3⁻CD4⁺ T_{conv} cells; **(B)** $\alpha 4$ and $\beta 1$ expression among CD44⁺ activated donor-derived CD8⁺ T cells and Foxp3⁻CD4⁺ T_{conv} cells; **(C)** Relative frequency of Foxp3⁺ T_{reg} cells among CD4⁺ donor-derived T cells. **(D)** Abundance of 1B11-reactive core 2 glycosylated CD43 among donor-derived CD4⁺ and CD8⁺ T cells, plotted as a function of staining with the pan-CD43-reactive S11 antibody. **(E)** Production of the inflammatory cytokines interferon (IFN)- γ and tumor necrosis factor (TNF)- α by donor-derived T cells after ex vivo restimulation with anti-CD3/CD28 antibodies. ns, not significant; *p<0.05, **p<0.01, ***p<0.001, ****p<0.0001 using one-way ANOVA with Tukey post-hoc test.

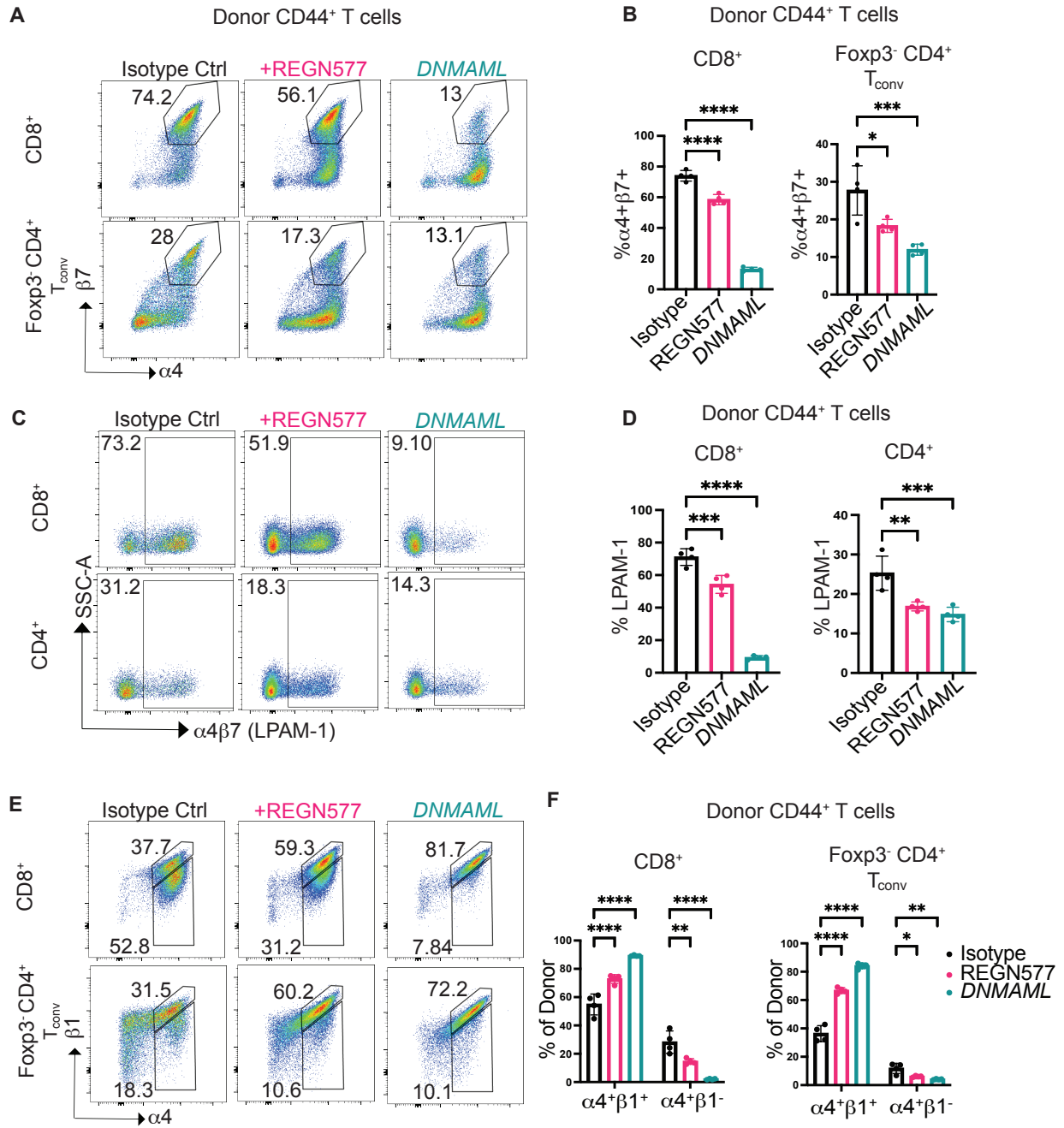


Figure S7. Both DNMAAML-mediated pan-Notch inhibition in T cells and systemic anti-DLL4 antibodies decrease $\alpha 4\beta 7$ expression in donor-derived conventional T cells after

allo-HCT in mice. Allo-HCT was performed using lethally irradiated C57BL/6 x BALB/c recipients (CBF1, 11 Gy) and C57BL/6 donors, with or without expression of the pan-Notch inhibitor DNMA1 in mature T cells (*Cd4-Cre;ROSA^{DNMA1}*, abbreviated DNMA1). Recipient groups were treated with isotype control or anti-mouse DLL4 (REGN577) antibodies (10 mg/kg i.p. at day 0 and day 2, n=4 per group, one of two representative experiments). **(A and B)** α 4 and β 7 expression among CD44⁺ activated donor-derived T cells in the spleen at day 4.5 after allo-HCT. Representative flow cytometry plots (A) and quantification (B) are shown for CD8⁺ and Foxp3⁻CD4⁺ T_{conv} cells; **(C and D)** α 4 β 7 dimer (LPAM-1) detection in activated donor-derived CD8⁺ and CD4⁺ T cells at day 4.5; representative plots (C) and quantification (D) are shown. **(E and F)** α 4 and β 1 expression in CD44⁺ activated donor-derived CD8⁺ T cells and Foxp3⁻CD4⁺ T_{conv} cells at day 4.5; representative plots (E) and quantification (F) are shown. *p<0.05, **p<0.01, ***p<0.001, ****p<0.0001 using one-way ANOVA with Tukey post-hoc test.

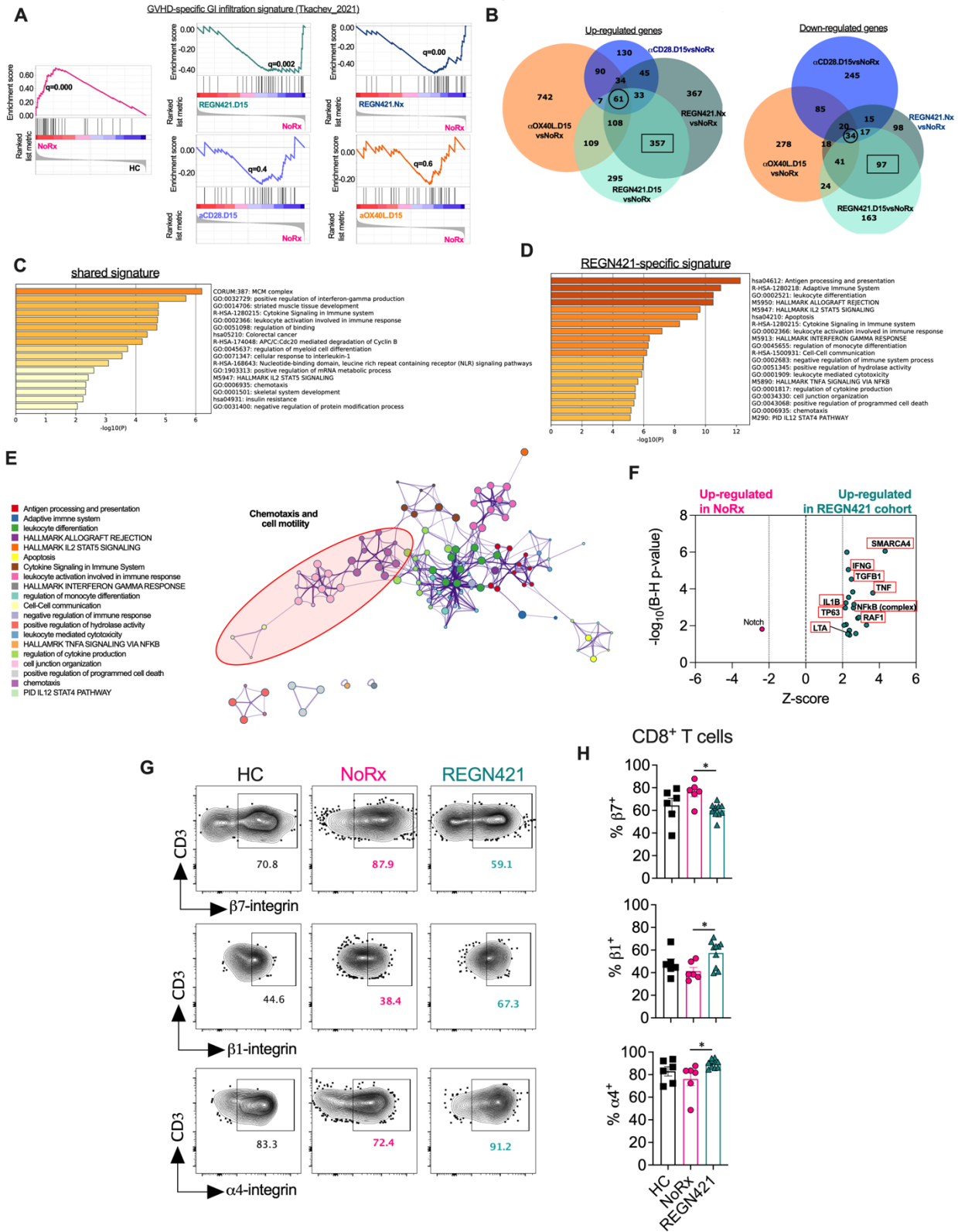


Figure S8. DLL4 blockade normalized the GVHD-specific T cell GI-infiltration signature and changed expression of individual integrin chains in NHPs. (A) Gene set enrichment

analysis (GSEA) plots showing enrichment for a recently defined GVHD-specific GI infiltration signature in untreated aGVHD (NoRx) compared to healthy controls (HC) and depicting normalization of this signature upon DLL4 inhibition, but not OX40L or CD28 blockade. **(B)** Venn diagram depicting the overlap of differentially expressed (DE) genes for each aGVHD cohort in comparison with NoRx aGVHD. Circled and boxed genes are evaluated further in **C** and **D**. **(C and D)** Functional annotation and pathway enrichment analysis was performed with 95 DE genes (61 over-represented, 34 under-represented; circled in Venn diagram **B**) that were affected by the three GVHD monoprophylaxis protocols in comparison with the NoRx aGVHD (the “shared signature”; **C**) and with 454 DE genes (357 over-represented, 97 under-represented; boxed in Venn diagram **B**) that were affected only by DLL4 blockade (the “REGN421-specific signature”, **D**) using the Metascape tool (Metascape.org). Top enriched ontology clusters are shown for each signature. **(E)** Visualization of top enriched functional pathways, as analyzed by hierarchical clustering and visualized using Metascape. The shaded area indicates a cluster of pathways associated with cell chemotaxis and mobility. **(F)** The 454 DE genes specifically affected by anti-DLL4 were analyzed using Ingenuity Pathway Analysis to identify upstream regulators activated or inhibited in the REGN421 aGVHD cohort relative to the NoRx aGVHD cohort. Shown are positive upstream regulators of *ITGB1* expression. B-H, Benjamini-Hochberg. **(G and H)**. Representative flow plots (**G**) and quantification (**H**) of α 4-integrin, β 1-integrin, and β 7-integrin subunit expression among spleen CD8⁺ T cells at day 15 after transplantation in allo-HCT recipients as compared to healthy controls (HC). Findings are shown for the untreated aGVHD (NoRx, n=6) and REGN421-treated (n=10) cohorts. *p<0.05 using one-way ANOVA with Tukey’s post-hoc test.

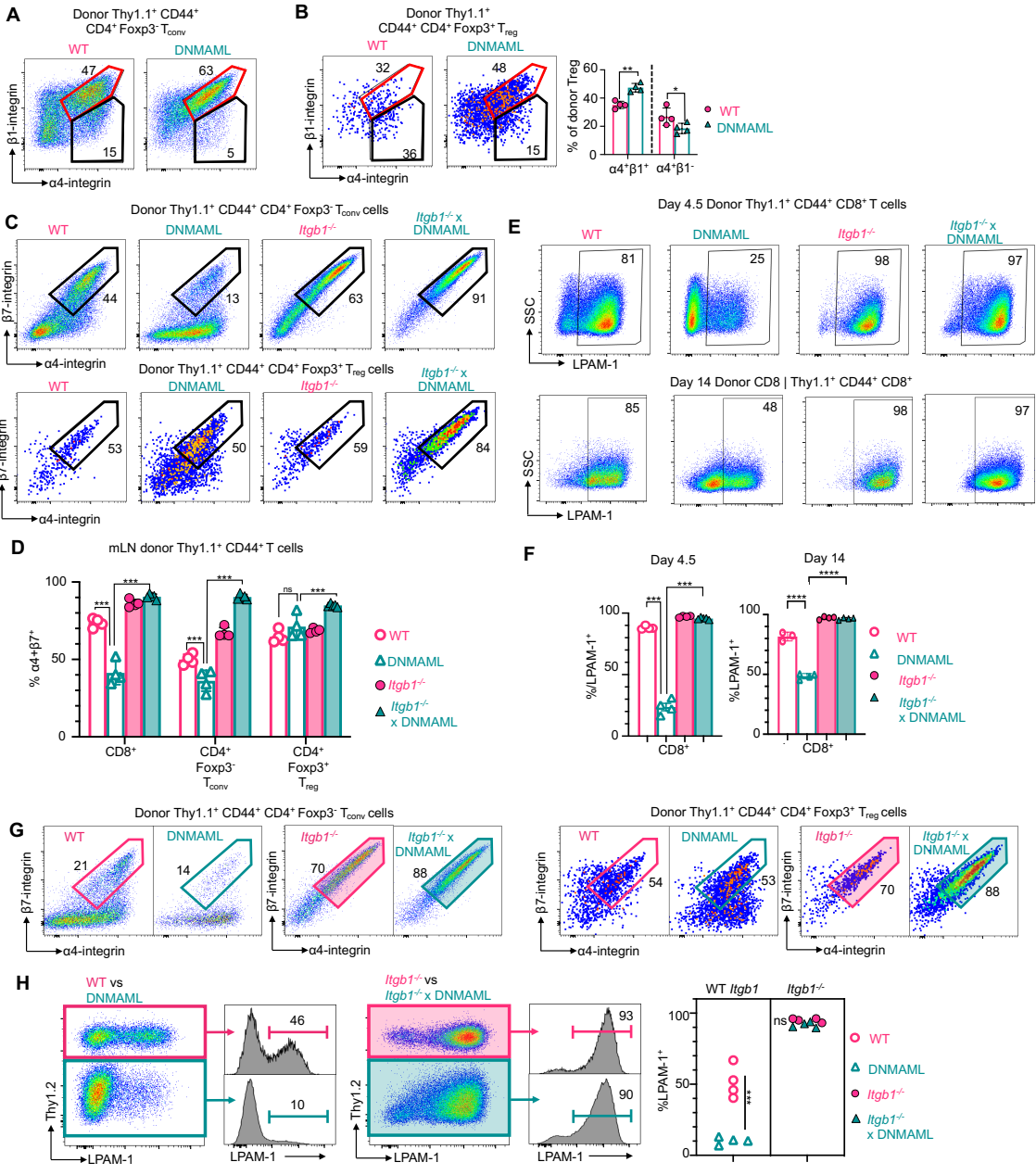


Figure S9. Loss of integrin $\beta 1$ rescues $\alpha 4\beta 7$ expression in Notch-deprived alloreactive T cells. (A to F) These data are related to the experiment depicted in Fig. 7C to G. (A and B) Representative flow plots showing $\alpha 4\beta 1$ expression among donor alloreactive $CD44^+CD4^+$ $Foxp3^- T_{conv}$ cells (A) and $Foxp3^+ T_{reg}$ cells (B). * $p < 0.05$, ** $p < 0.01$, two-way ANOVA with Tukey's post-hoc tests (C) Representative flow cytometry plots showing $\alpha 4\beta 7$ expression in $CD4^+ T_{conv}$ (top) and T_{reg} (bottom) cells represented as summary data in Fig. 7G. (D) Summary data of $\alpha 4\beta 7$ expression in donor T cell subsets harvested from mesenteric lymph nodes (mLN). *** $p < 0.001$, two-way ANOVA with Tukey's post-hoc tests. ns, not significant. (E and F)

Representative flow cytometry plots (E) depicting the impact of *Itgb1* loss on expression of the $\alpha 4\beta 7$ /LPAM-1 heterodimer among donor-derived CD8⁺ cells at day 4.5 (top) and day 14 (bottom) after allo-HCT (spleen), with quantification (F). *** $p < 0.001$, **** $p < 0.0001$, one-way ANOVA with Tukey's post-hoc tests. **(G and H)** Related to experiment from Fig. 7H and I. **(G)** Representative flow cytometry plots of cell surface $\alpha 4\beta 7$ in competing donor CD4⁺ T_{conv} (left) and T_{reg} (right) subsets as summarized in Fig. 7I. **(H)** Representative flow cytometry plots and summary data of $\alpha 4\beta 7$ /LPAM-1 abundance in competing donor CD8⁺ T cells. $n = 4$ mice per group for both experiments. *** $p < 0.001$, two-way ANOVA with Tukey's post-hoc tests. ns, not significant.

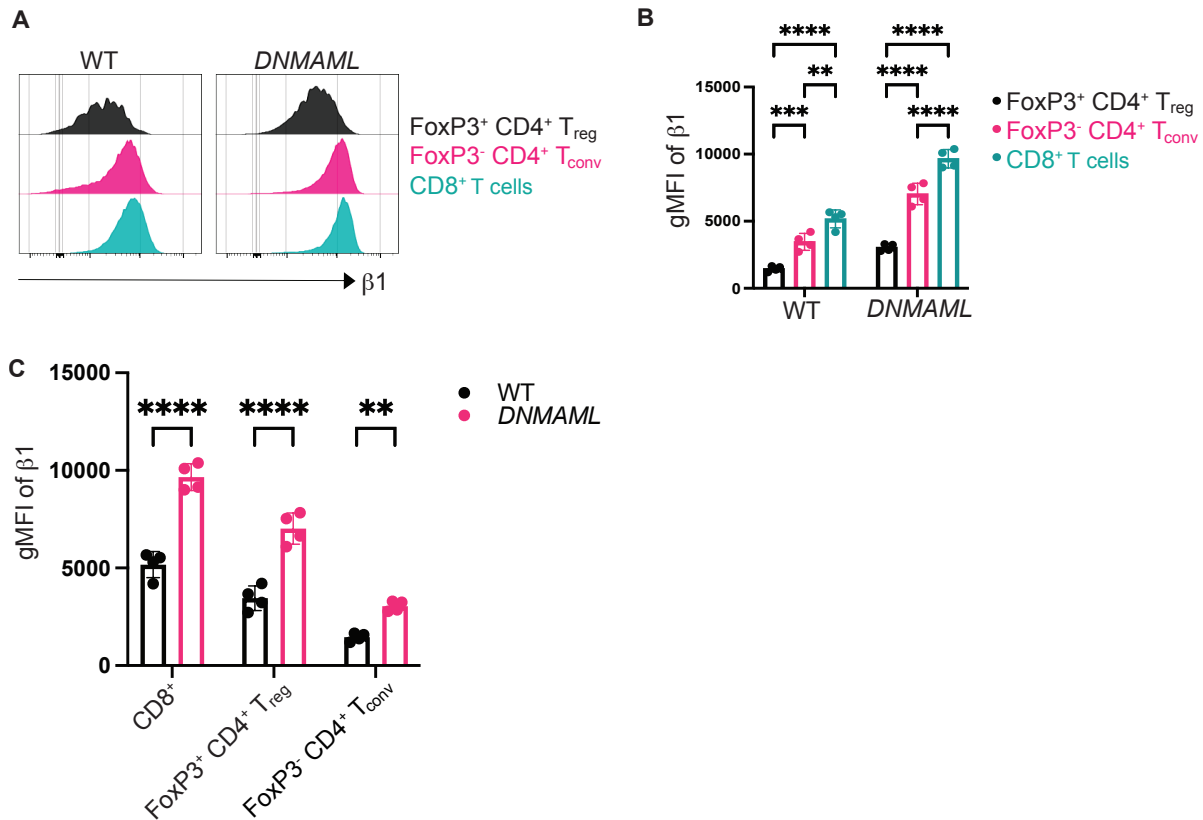


Figure S10. Differential abundance of surface $\beta 1$ integrin among T cell subsets after allo-HCT. Allo-HCT was performed using lethally irradiated C57BL/6 x BALB/c recipients (CBF1, 11 Gy) and C57BL/6 donors with or without expression the pan-Notch inhibitor DNMAHL in mature T cells (WT versus DNMAHL, $n=4$ recipients per group). At day 4.5 after allo-HCT, the relative abundance of surface $\beta 1$ integrin was assessed among CD44⁺ donor-derived Foxp3⁺ CD4⁺ T_{reg} cells, Foxp3⁻ CD4⁺ T_{conv} cells and CD8⁺ T cells. **(A and B)** Representative flow cytometry histograms (A) with geometric mean fluorescence intensity (gMFI) quantified (B). **(C)** Direct comparison of surface $\beta 1$ expression in individual T cell subsets as a function of DNMAHL-mediated Notch inhibition. ** $p < 0.01$, *** $p < 0.001$, **** $p < 0.0001$ using one-way ANOVA with Tukey post-hoc test.

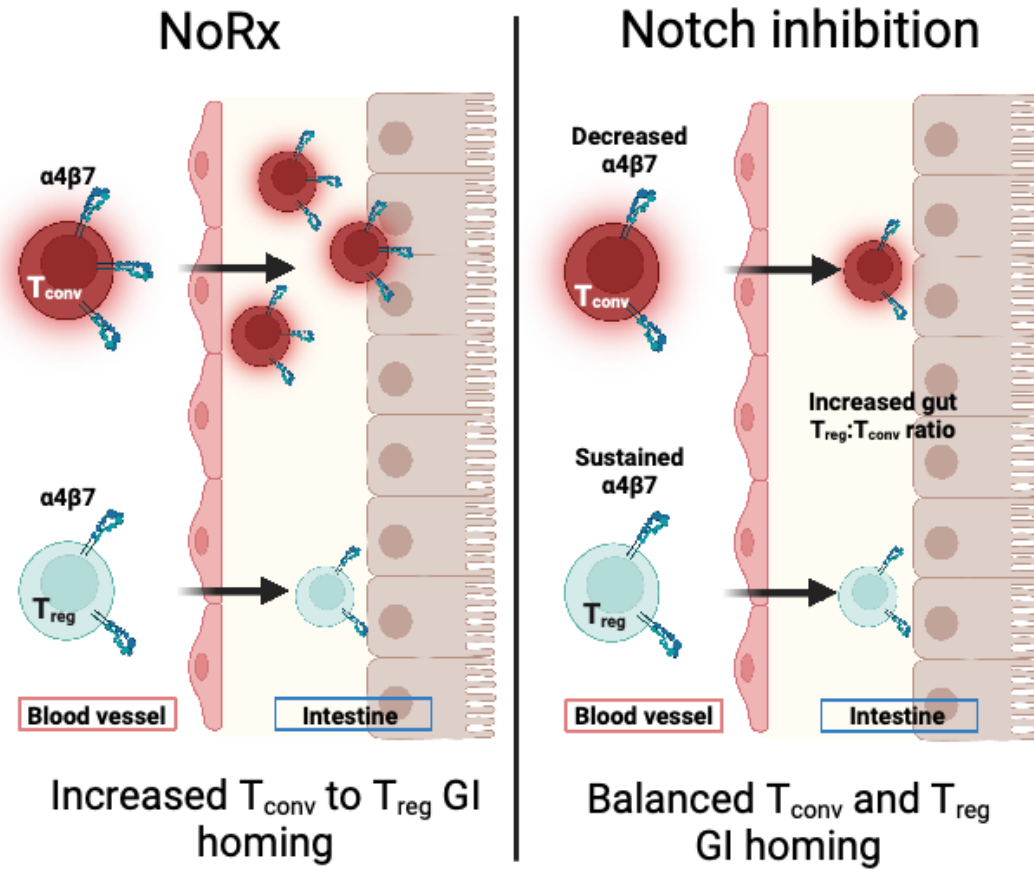


Figure S11. Working model depicting how inhibition of Notch signaling in T cells differentially affects cell surface $\alpha 4\beta 7$ /LPAM-1 in T_{conv} and T_{reg} cells, resulting in decreased T_{conv} gut infiltration and an increased gut $T_{reg}:T_{conv}$ ratio early after allo-HCT.

Supplementary Data Files

Data file S1. Transplant characteristics and data inclusion.

Data file S2. List of differentially expressed genes.

Data file S3. List of differentially expressed genes (aDLL4-specific).

Data file S4. aDLL4-aOX40L-aCD28 shared differentially expressed genes.

Data file S5. Shared signature pathway enrichment analysis.

Data file S6. aDLL4 signature pathway enrichment analysis.

Data file S7. aDLL4 signature upstream regulators.

Data file S8. List of critical reagents.

Data file S9. Raw, individual-level data for experiments where $n < 20$.